Cover sheet

Authors: Xiu-Xiu Ma, Xu-Hong Dai, Xing-Quan He

Manuscript title: Co_9S_8 Modified N, S, and P Ternary-Doped 3D Graphene Aerogels as A High Performance Electrocatalyst for both Oxygen Reduction Reaction and Oxygen Evolution Reaction

Number of pages, figures, and tables in the manuscript was 30, 6, and 0, respectively.

Number of pages, figures, and tables in the supporting information was 17, 8, and 5, respectively.

Supporting Information

Co_9S_8 Modified N, S, and P Ternary-Doped 3D Graphene Aerogels as A High Performance Electrocatalyst for both Oxygen Reduction Reaction and Oxygen Evolution Reaction

Xiu-Xiu Ma[a], Xu-Hong Dai[a], Xing-Quan He[a]*[1]

[a]*School of Materials Science and Engineering, Changchun University of Science and Technology, Weixing Road, No. 7989, Changchun, 130022, Jilin, R.P. China.*

[1] *Corresponding author: hexingquan@hotmail.com (X.Q. He)

Tel: + 86 8558 343

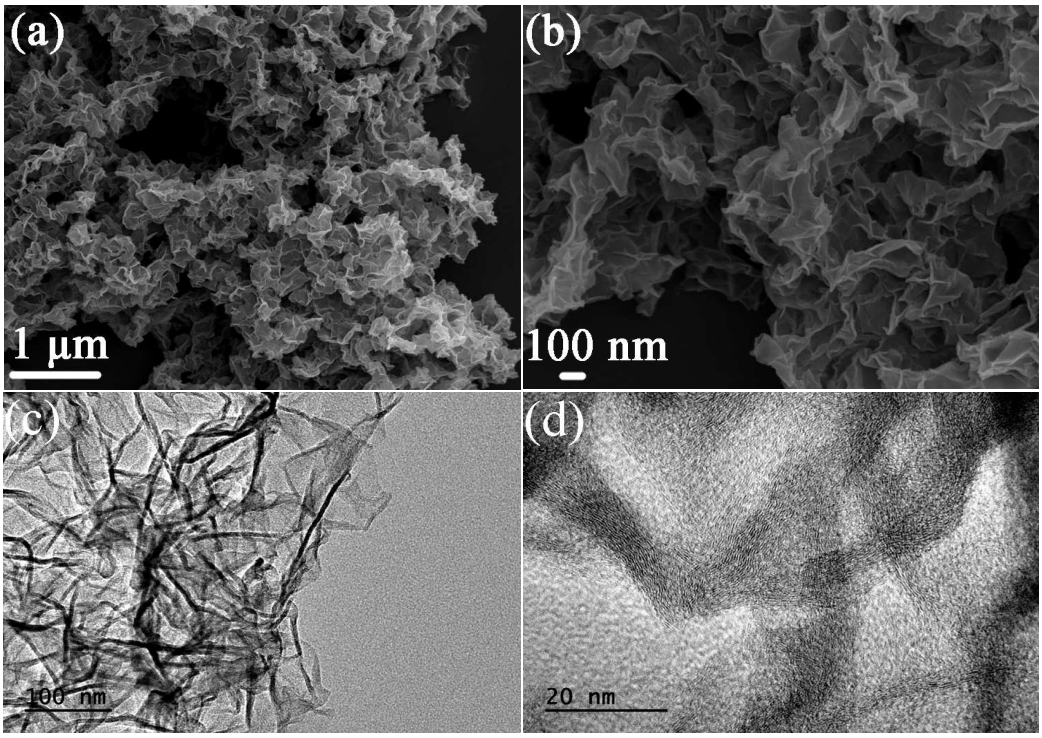

Figure S1. (a) Low and (b) high magifition SEM images of NSPG-900. (c) TEM and (d) HRTEM images of NSPG-900.

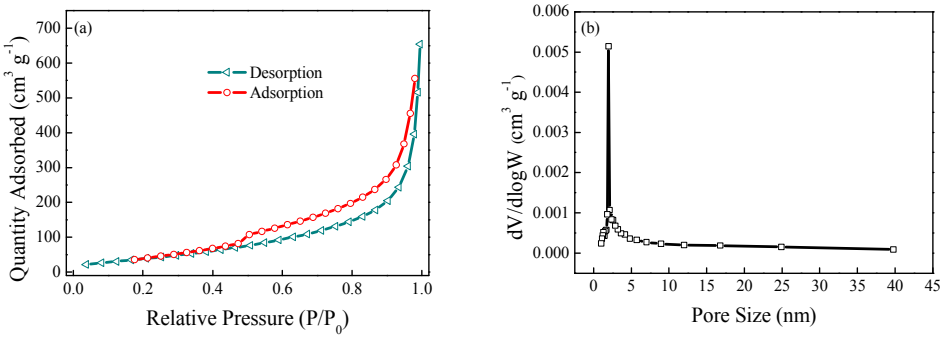

Figure S2. (a) N_2 adsorption-desorption isotherms and (b) the corresponding BJH pore size distribution curves of NSPG-900.

Table S1. Specific BET surface area, pore size and pore volume of the investigated catalysts

Catalyst	S_{BET} (m^2 g^{-1})	Pore size (nm)	Pore volume (cm^3 g^{-1})
NSPG-900	657	5.6	0.10
Co_9S_8/NSPG-800	436	4.8	0.15
Co_9S_8/NSPG-900	478	6.1	0.13
Co_9S_8/NSPG-1000	300	5.1	0.06

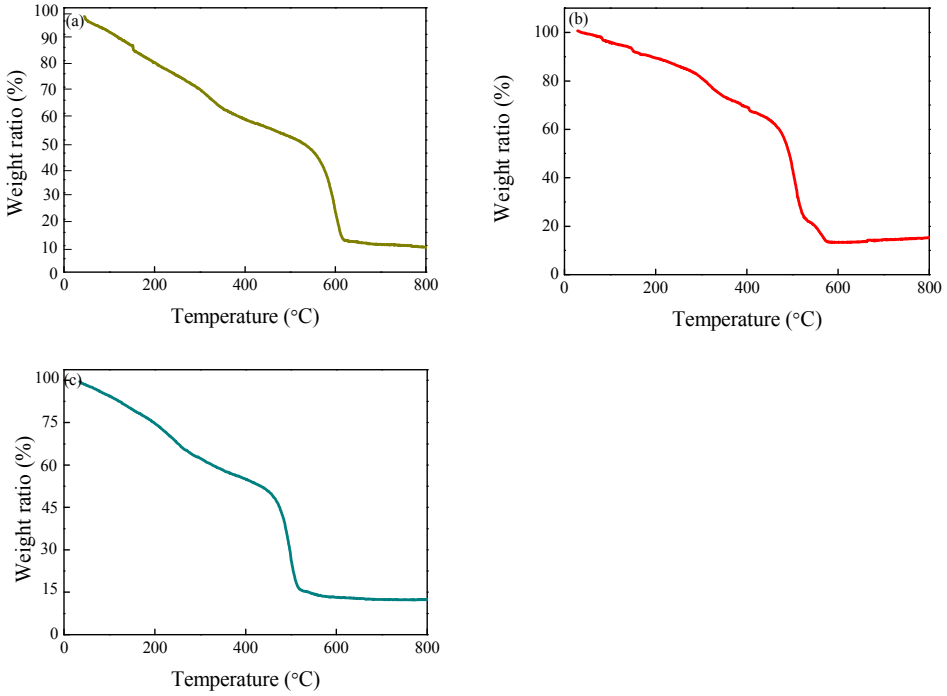

Figure S3. TGA curves of (a) Co_9S_8/NSPG-800, (b) Co_9S_8/NSPG-900 and (c) Co_9S_8/NSPG-1000 under air atmosphere.

Table S2. Elemental contents of C, O, N, S, P and Co in the samples determined by XPS analysis

Catalyst	C (at%)	O (at%)	N (at%)	S (at%)	P (at%)	Co (at%)
NSG-900	90.41	6.46	2.11	1.02	-	-
Co_9S_8/NSPG-800	90.32	6.56	2.56	0.86	0.15	0.41
Co_9S_8/NSPG-900	91.80	4.48	2.28	0.99	0.13	0.32
Co_9S_8/NSPG-1000	92.35	4.37	2.09	0.79	0.11	0.29

Table S3. The relative percentages of deconvoluted S 2p, N 1s and P 2p species in Co_9S_8/NSPG-800, Co_9S_8/NSPG-900, and Co_9S_8/NSPG-1000

Species	Co_9S_8/NSPG-800	Co_9S_8/NSPG-900	Co_9S_8/NSPG-1000
S $2p_{3/2}$	45.67%	37.65%	50.10%
S $2p_{1/2}$	41.52%	49.88%	39.28%
Thiophene S	5.88%	6.61%	5.61%
SO_x	6.92%	5.86%	5.01%
Pyrrolic N	21.31%	15.62%	13.58%
Pyridinic N	23.50%	21.08%	19.09%
Graphitic N	37.41%	42.23%	43.85%
Oxidized N	17.78%	21.07%	23.48%
P-C	31.18%	17.61%	30.43%
P-N	34.51%	19.37%	21.75%
C-O-PO_3	34.31%	63.03%	47.82%

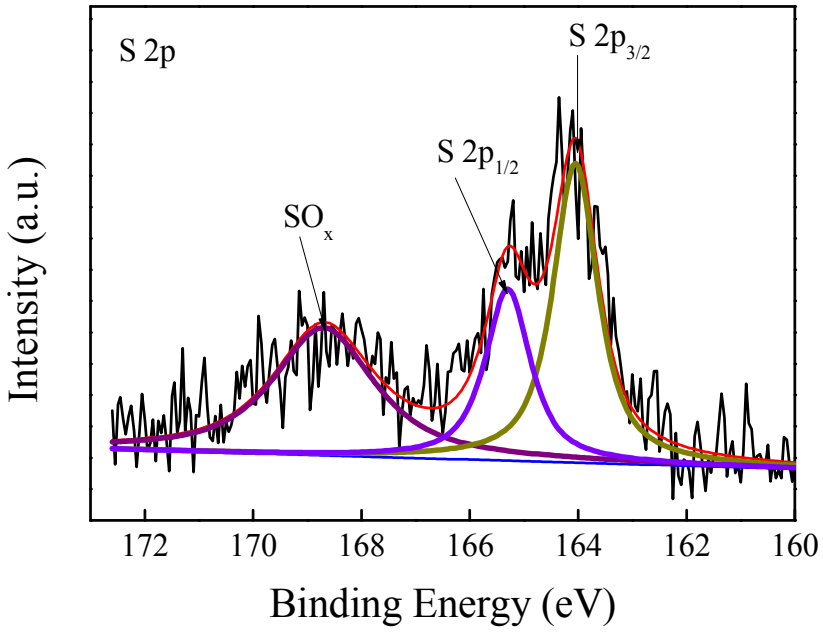

Figure S4. High resolution XPS of S 2p in NSG.

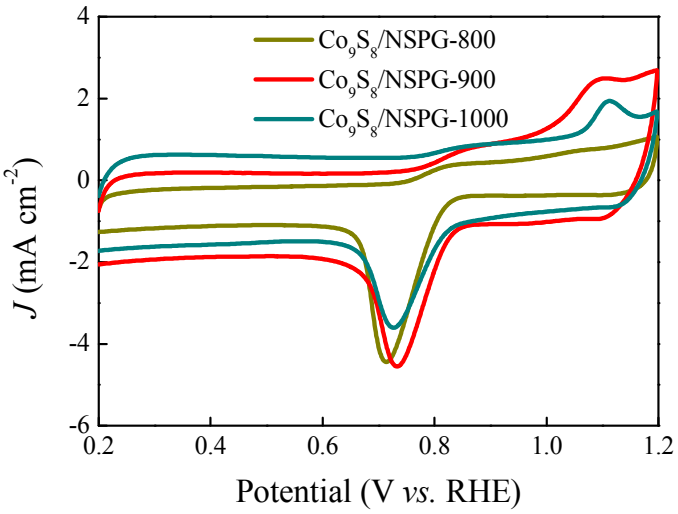

Figure S5. Cyclic voltammetry curves of Co_9S_8/NSPG-800, Co_9S_8/NSPG-900 and Co_9S_8/NSPG-1000 for ORR.

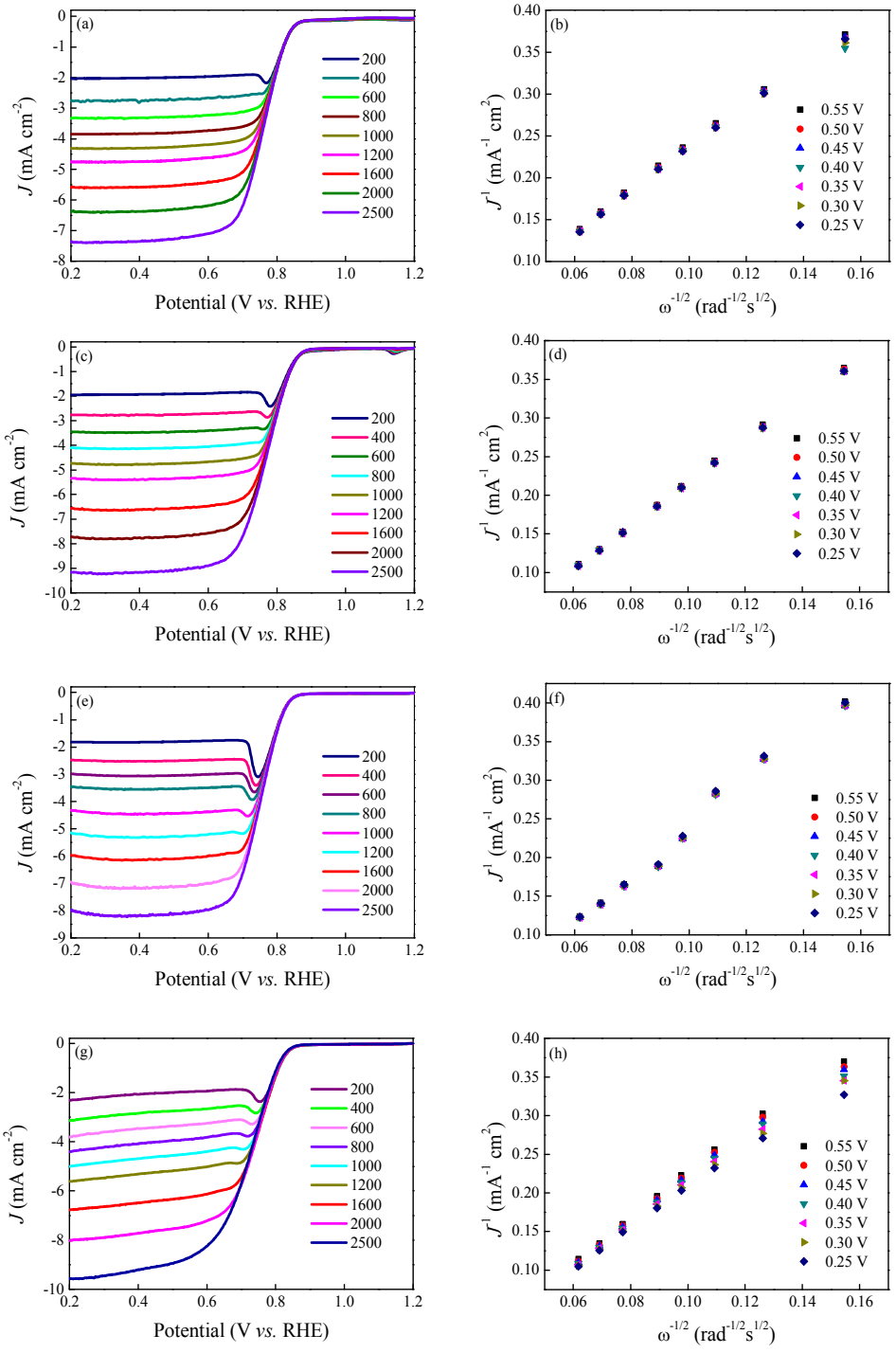

Figure S6. (a, c, e, g) Linear sweep voltammetry curves of NSPG-900 (a), Co_9S_8/NSG-900 (c), Co_9S_8/NSPG-800 (e), and Co_9S_8/NSPG-1000 (g). (b, d, f, h) Corresponding K-L plots of NSPG-900 (b), Co_9S_8/NSG-900 (d), Co_9S_8/NSPG-800 (f), and Co_9S_8/NSPG-1000 (h).

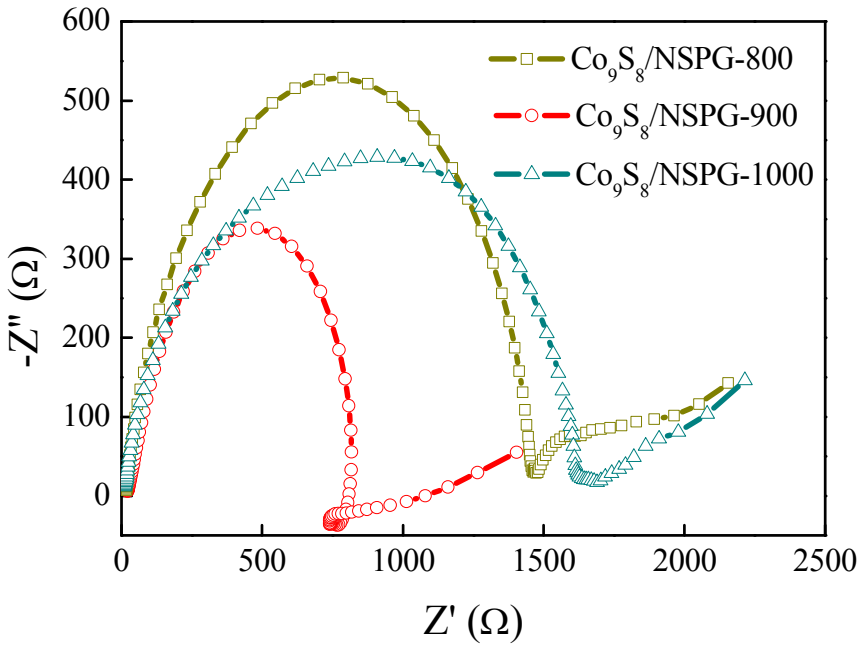

Figure S7. AC Nyquist electrochemical impedance plots of Co_9S_8/NSPG, Co_9S_8/NSPG-900 and Co_9S_8/NSPG-1000.

Table S4. ORR parameters of Co_9S_8/NSPG-900 compared to catalysts in literatures

Catalysts	$E_{1/2}$ [V *vs.* RHE]	J_L [mA cm^{-2}]	Tafel slope [mV dec^{-1}]	References
Co_9S_8/NSPG-900	0.800	7.26	79	This work
20 wt% Pt/C	0.830	5.47	84	This work
Co_9S_8/N-C	0.784	5.46	69	[1]
Co_9S_8/NPCP@rGO	0.784	5.40	62	[2]
CoxSy@C-1000	0.814	4.70	–	[3]
CoS_2(400)/N,S-GO	0.790	4.70	30	[4]
SN-rGO	0.797	3.13	67	[5]
$Co_3(PO_4)_2$C-N/rGOA	0.837	3.72	35	[6]
$Co_3(PO_4)_2$	0.670	5.20	–	[7]
FeP@NPCs	0.820	5.85	78	[8]
Fe–Nx/C	0.920	6.17	–	[9]
FePPyC-900	0.814	6.40	78	[10]

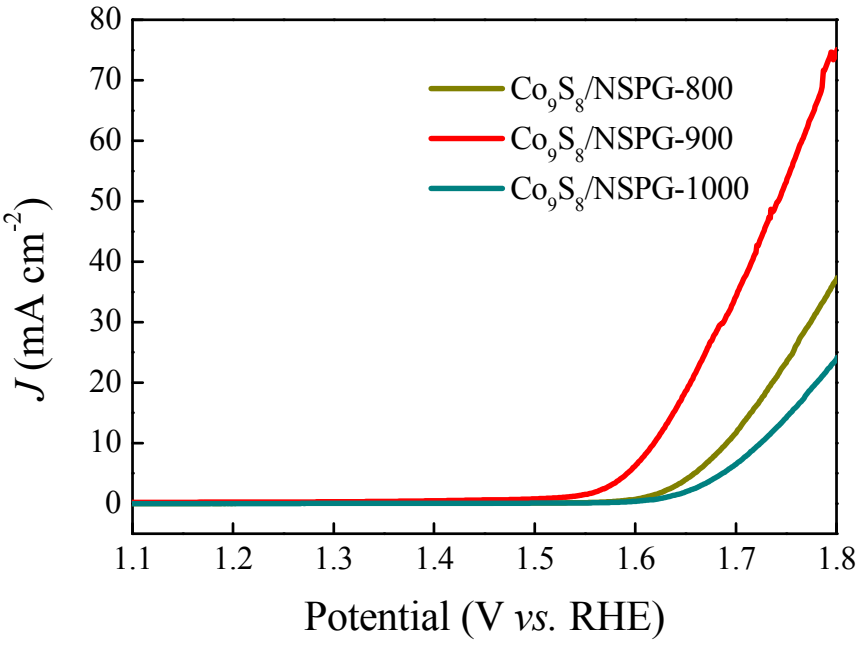

Figure S8. LSV curves of Co_9S_8/NSPG, Co_9S_8/NSPG-900 and Co_9S_8/NSPG-1000 for OER on a RDE at 1600 rpm and 10 mV s^{-1} in O_2-saturated 1.0 M KOH.

Table S5. OER parameters of Co_9S_8/NSPG-900 compared to catalysts in literatures

Catalysts	η_{10} [mV]	Tafel slope [mV dec^{-1}]	Reference
Co_9S_8/NSPG-900	343	82	This work
RuO_2	370	79	This work
Co_9S_8/N-C	371	75	[1]
Co_xS_y@C-1000	470	–	[3]
CoS_2(400)/N,S-GO	380	75	[4]
FeP@NPC	300	80	[8]
Fe_3O_4/Co_3S_4	210	–	[11]
CNT-CoS_2	290	255	[12]
Co_9S_8@CoS@CoO@C	150	96	[13]
Fe_3O_4@Co_9S_8/rGO	340	55	[14]
CoNi-LDH/Fe-PPLBL	264	38	[15]
Co_9S_8@MoS_2/CNFs	340	61	[16]

Reference

[1] Cao, X.; Zheng, X.; Tian, J.; Jin, C.; Ke, K.; Yang, R. Cobalt Sulfide Embedded in Porous Nitrogen-doped Carbon as a Bifunctional Electrocatalyst for Oxygen Reduction and Evolution Reactions. Electrochimica Acta **2016**, *191*, 776–783.

[2] Liu, Y.; Shen, H.; Jiang, H.; Li, W.; Li, J.; Li, Y.; Guo, Y. ZIF-Derived Graphene Coated/Co_9S_8 Nanoparticles Embedded in Nitrogen Doped Porous Carbon Polyhedrons as Advanced Catalysts for Oxygen Reduction Reaction. International Journal of Hydrogen Energy **2017**, *42*, 12978–12988.

[3] Chen, B.; Li, R.; Ma, G.; Gou, X.; Zhu, Y.; Xia, Y. Cobalt Sulfide/N,S Codoped Porous Carbon Core–Shell Nanocomposites as Superior Bifunctional Electrocatalysts for Oxygen Reduction and Evolution Reactions. Nanoscale **2015**, *7*, 20674–20684.

[4] Ganesan, P.; Prabu, M.; Sanetuntikul, J.; Shanmugam, S. Cobalt Sulfide Nanoparticles Grown on Nitrogen and Sulfur Codoped Graphene Oxide: An Efficient Electrocatalyst for Oxygen Reduction and Evolution Reactions. ACS Catal. **2015**, *5*, 3625−3637.

[5] Bag, S.; Mondal, B.; Das, A.; Raj, C. Nitrogen and Sulfur Dual-Doped Reduced Graphene Oxide: Synergistic Effect of Dopants towards Oxygen Reduction Reaction. Electrochimica Acta **2015**, *163*, 16–23.

[6] Zhou, T.; Du, Y.; Yin, S.; Tian, X.; Yang, H.; Wang, X.; Liu, B.; Zheng, H.; Qiao, S.; Xu, R. Nitrogen-Doped Cobalt Phosphate@Nanocarbon Hybrids for Efficient Electrocatalytic Oxygen Reduction. Energy Environ. Sci. **2016**, *9*, 2563–2570.

[7] Senthilkumar, B.; Khan, Z.; Park, S.; Seo, I.; Ko, H.; Kim, Y. Exploration of

Cobalt Phosphate as a Potential Catalyst for Rechargeable Aqueous Sodium-Air Battery. Journal of Power Sources **2016**, *311*, 29–34.

[8] Zhang, R.; Zhang, C.; Chen, W. FeP Embedded in N, P Dual-Doped Porous Carbon Nanosheet: An Efficient and Durable Bifunctional Catalyst for Oxygen Reduction and Evolution Reactions. J. Mater. Chem. A **2016**, *4*, 18723–18729.

[9] Zhao, Y.; Kamiya, K.; Hashimoto, K.; Nakanishi, S. Efficient Oxygen Reduction Reaction Electrocatalysts Synthesized from An Iron Coordinated Aromatic Polymer Framework. J. Mater. Chem. A **2016**, *4*, 3858–3864.

[10] Tran, T.; Song, M.; Singh, K.; Yang, D.; Yu, J. Iron–Polypyrrole Electrocatalyst with Remarkable Activity and Stability for ORR in both Alkaline and Acidic Conditions: A Comprehensive Assessment of Catalyst Preparation Sequence. J. Mater. Chem. A **2016**, *4*, 8645–8657.

[11] Du, J.; Zhang, T.; Xing, J.; Xu, C. Hierarchical Porous Fe_3O_4/Co_3S_4 Nanosheets as Efficient Electrocatalysts for Oxygen Evolution Reaction. J. Mater. Chem. A **2017**, *5*, 9210–9216.

[12] Yang, J.; Yang, Z.; Li, L.; Cai, Q.; Nie, H.; Ge, M.; Chen, X.; Chen, Y.; Huang, S. Highly Efficient Oxygen Evolution from CoS_2/CNT Nanocomposites via a One-Step Electrochemical Deposition and Dissolution Method. Nanoscale **2017**, *9*, 6886–6894.

[13] Long, Y.; Gong, Y.; Lin, J. Metal–Organic–Framework–Derived Co_9S_8@CoS@CoO@C Nanoparticles as Efficient Electro- and Photo-Catalysts for Oxygen Evolution Reaction. J. Mater. Chem. A **2017**, *5*, 10495–10509.

[14] Yang, J.; Zhu, G.; Liu, Y.; Xia, J.; Ji, Z.; Shen, X.; Wu, S. Fe_3O_4-Decorated Co_9S_8 Nanoparticles In Situ Grown on Reduced Graphene Oxide: A New and Efficient Electrocatalyst for Oxygen Evolution Reaction. Adv. Funct. Mater. **2016**, *26*, 4712–4721.

[15] Zhang, C.; Zhao, J.; Zhou, L.; Li, Z.; Shao, M.; Wei, M. Layer-By-Layer Assembly of Exfoliated Layered Double Hydroxide Nanosheets for Enhanced Electrochemical Oxidation of Water. J. Mater. Chem. A **2016**, *4*, 11516–11523.

[16] Zhu, H.; Zhang, J.; Yanzhang, R.; Du, M.; Wang, Q.; Gao, G.; Wu, J.; Wu, G.; Zhang, M.; Li, B.; Yao, J.; Zhang, X. When Cubic Cobalt Sulfide Meets Layered Molybdenum Disulfide: A Core–Shell System Toward Synergetic Electrocatalytic Water Splitting. Adv. Mater. **2015**, *27*, 4752–4759.